*Geophysical Prospecting,* 2003, **51**, 381–392

# Modelling frequency-dependent seismic anisotropy in fluid-saturated rock with aligned fractures: implication of fracture size estimation from anisotropic measurements

Sonja Maultzsch, Mark Chapman, Enru Liu* and Xiang Yang Li

*British Geological Survey, Murchison House, West Mains Road, Edinburgh EH9 3LA, UK*

Received July 2002, revision accepted April 2003

**ABSTRACT**

Measurements of seismic anisotropy in fractured rock are used at present to deduce information about the fracture orientation and the spatial distribution of fracture intensity. Analysis of the data is based upon equivalent-medium theories that describe the elastic response of a rock containing cracks or fractures in the long-wavelength limit. Conventional models assume frequency independence and cannot distinguish between microcracks and macrofractures. The latter, however, control the fluid flow in many subsurface reservoirs. Therefore, the fracture size is essential information for reservoir engineers. In this study we apply a new equivalent-medium theory that models frequency-dependent anisotropy and is sensitive to the length scale of fractures. The model considers velocity dispersion and attenuation due to a squirt-flow mechanism at two different scales: the grain scale (microcracks and equant matrix porosity) and formation-scale fractures. The theory is first tested and calibrated against published laboratory data. Then we present the analysis and modelling of frequency-dependent shear-wave splitting in multicomponent VSP data from a tight gas reservoir. We invert for fracture density and fracture size from the frequency dependence of the time delay between split shear waves. The derived fracture length matches independent observations from borehole data.

## INTRODUCTION

Fractures are common geological features in the subsurface of the earth's crust, and they control much of the mechanical strength and transport properties of the solid structure. Fracture systems are also crucial for hydrocarbon production, control and manipulation of water supplies, and dispersal of pollutants. Much of our knowledge about the earth's crust is obtained from seismic waves. One of the most successful methods for the detection and characterization of fractures and the prediction of fluid-flow directions is the use of seismic shear waves (Crampin 1985; Queen and Rizer 1990; Li 1997). The success of seismic anisotropy is its ability to provide subsurface fracture orientations as derived from the polarization of fast shear waves, and spatial distribution of fracture intensity inferred from time delays between fast and slow shear waves. However, the reservoir engineers' reluctance to accept seismic anisotropy as a routine technique for fracture characterization is partially because of its failure to provide information about sizes and volume of fractures. So far the terms 'crack' and 'fracture' have been used as synonyms in geophysics and we do not distinguish between microcracks and macrofractures. Although it has been thought that both micro-scale (grain-scale) cracks and/or macro-scale (metre-scale) fractures can be considered the dominant causes of observed anisotropy in hydrocarbon reservoirs (Liu *et al*. 1993), reservoir engineers are more interested in the latter as fluid flow in reservoirs is believed to be dominated by large-scale fluid units (Queen, Rizer and DeMartini 1992). Therefore, a quantitative

*E-mail: e.liu@bgs.ac.uk

characterization of natural fracture systems in the subsurface from seismic data would potentially provide essential information for the prediction of permeability and flow patterns within reservoirs.

In the long-wavelength limit, the elastic response of a fractured rock is described by equivalent-medium theories. Various theories have been developed (e.g. Schoenberg 1980; Hudson 1981; Nishizawa 1982; Thomsen 1995). These models predict frequency-independent behaviour and are in that sense static equivalent-medium theories. There is agreement between the models for dry rock, but considerable differences occur in the case of fluid fill and fluid flow between cracks and pores (Liu, Hudson and Pointer 2000).

For applications to seismic data, the Thomsen equant porosity model (Thomsen 1995) and the Hudson model (Hudson 1981) are most widely used. Thomsen's model assumes perfect pressure equalization between cracks and equant pores in the surrounding rock matrix. It is therefore limited to low frequencies, where the period of the wave is much longer than the time it takes for the pressure to equalize. The flow of fluid from cracks into equant pores can significantly increase the anisotropy (Thomsen 1995). In contrast, Hudson's model (Hudson 1981) assumes that cracks are isolated and that there is no fluid communication between elements of pore space. It can thus be regarded as a high-frequency theory, bearing in mind that it is still only valid when wavelengths are much longer than the length scale associated with the cracks.

A common parameter in all theories, which is related to the magnitude of anisotropy, is the crack density $\varepsilon$. It is defined as the number density $\gamma$ of cracks multiplied by the crack radius $a$ cubed: $\varepsilon = \gamma a^3$. The crack density can be estimated from the time delay of split shear waves (Crampin 1985; Mueller 1992; Li 1997; Potters *et al*. 1999). However, a material with only a few large fractures can have the same crack density as a material with many small cracks, which is schematically illustrated in Fig. 1. Thus, conventional equivalent-medium theory cannot determine whether the anisotropy is caused by microcracks or by macrofractures that would potentially enhance fluid flow in hydrocarbon reservoirs.

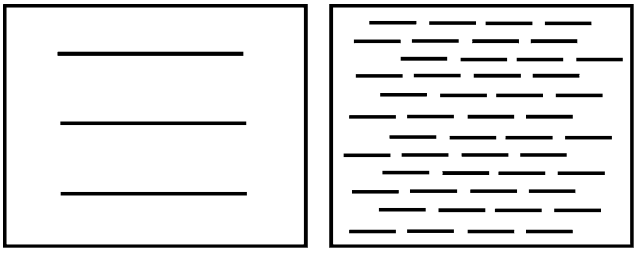

**Figure 1** The same crack density can be caused by a few large fractures as shown on the left or many small cracks as shown on the right.

Some results obtained from data cannot be explained by static equivalent-medium theory and demand the use of more complicated models. Van der Kolk, Guest and Potters (2001) found that a region with a large increase in shear-wave splitting and attenuation of high frequencies coincided with the gas/oil contact in a fractured carbonate reservoir. Furthermore, there is evidence that anisotropy can depend on frequency: Marson-Pidgeon and Savage (1997) and Liu *et al*. (2001) observed a decrease in time delay between split shear waves with increasing frequency in earthquake data.

Dynamic equivalent-medium theories have been proposed by Hudson, Liu and Crampin (1996; interconnected crack model and equant porosity model) and van der Kolk *et al*. (2001; BOSK model). Tod (2001) considered the Hudson interconnected crack model in the case of nearly aligned cracks. For application purposes these models have limitations. It is not possible to remove the fractures from the models and then calibrate them against laboratory data. Furthermore, the explanation of observed effects in the seismic frequency range can be problematic.

In this study, we use a poroelastic model recently proposed by Chapman (2003). The model considers two different length scales: a grain scale with microcracks and equant pores and a scale larger than that with aligned fractures. It describes frequency-dependent anisotropy with the length of the fractures being one of the key parameters. The model is first tested and calibrated against published laboratory data. Then we apply the calibrated theory to model frequency-dependent anisotropy that has been observed in multicomponent VSP data. The measured change in time delay between split shear waves with frequency is used to invert for fracture density and fracture size. We test the results with synthetic modelling. Finally, the derived fracture length is compared with independent borehole data.

## THEORETICAL MODEL

The poroelastic model of Chapman (2003) is based on a squirt-flow mechanism in fractured porous rock. It considers an isotropic collection of spherical pores and ellipsoidal microcracks, the size of which is identified with the grain scale, and the presence of aligned fractures, which can be larger than the grain scale. Thus, the theory accounts for two different length scales. The resulting medium is transversely isotropic.

The model agrees with the results of Brown and Korringa (1975) and Hudson (1981) in the low- and high-frequency

limits, respectively. In the absence of fractures it returns to the earlier squirt-flow model of Chapman, Zatsepin and Crampin (2002). Tests of this earlier model against laboratory measurements are discussed by Chapman (2000).

The expressions for the elements of the effective stiffness tensor are given by Chapman (2003). The stiffness tensor is of the form:

$$C_{ijkl} = C^0_{ijkl} - \Phi_p C^1_{ijkl} - \varepsilon_c C^2_{ijkl} - \varepsilon_f C^3_{ijkl}, \quad (1)$$

where $\mathbf{C}^0$ is the isotropic elastic tensor of the matrix with Lamé parameters $\lambda$ and $\mu$; $\mathbf{C}^1$, $\mathbf{C}^2$ and $\mathbf{C}^3$ are the additional contributions from pores, microcracks and fractures, respectively, multiplied by the porosity $\Phi_p$, the crack density $\varepsilon_c$, and the fracture density $\varepsilon_f$. The corrections are functions of the Lamé parameters, fluid and fracture properties, frequency, and a time-scale parameter $\tau$, which is related to the squirt flow.

Since the calculation of the elastic constants followed the interaction energy approach of Eshelby (1957), the model in its original form is restricted to very low porosity. To circumvent the problem, we use a slightly modified version as described by Chapman *et al*. (2003). The method is similar to the self-consistent scheme. We suggest using Lamé parameters $\lambda^o$ and $\mu^o$ for the corrections that are derived from the velocities $V_p^o$ and $V_s^o$ of the unfractured porous rock. Additionally, we require $\mathbf{C}^0(\Lambda, M)$ to be defined in such a way that the measured isotropic velocities are obtained by applying the crack and pore correction at a certain frequency $f_0$. Therefore, we must have

$$\Lambda = \lambda^o + \Phi_{c,p}(\lambda^o, \mu^o, f_0), \; \mathrm{M} = \mu^o + \Phi_{c,p}(\lambda^o, \mu^o, f_0), \quad (2)$$

with $\lambda^o = \rho\,(V_p^o)^2 - 2\mu^o$ ; $\mu^o = \rho(V_s^o)^2$.

Equation (1) is then written as

$$C_{ijkl}(\omega) = C^0_{ijkl}(\Lambda, \mathrm{M}, \omega) - \Phi_p C^1_{ijkl}(\lambda^o, \mu^o, \omega) - \varepsilon_c C^2_{ijkl}(\lambda^o, \mu^o, \omega) - \varepsilon_f C^3_{ijkl}(\lambda^o, \mu^o, \omega). \quad (3)$$

Now the corrections for pores, microcracks and fractures, which describe the frequency dependence and anisotropy of the material, will be calculated with physical properties obtained from measured velocities instead of being fitted to the data.

Chapman *et al*. (2003) have shown that in cases of high porosity the model can be further simplified by setting the microcrack density $\varepsilon_c$ to zero. The influence of the parameter is negligible for modelling the effect of fractures, if the spherical porosity is significantly larger than the crack porosity. This will be the case for most practical applications, and therefore the number of variables can be further reduced.

The fact that fluid flow in the model takes place at two scales, the grain scale (microcracks and pores) and the fracture scale, leads to the existence of two characteristic frequencies and associated relaxation times. The grain-scale fluid flow is related to the traditional squirt-flow frequency (or relaxation time $\tau_m$), which experiments suggest lie somewhere between the sonic and ultrasonic range (Murphy 1985; Winkler 1986; Lucet and Zinszner 1992; Thomsen 1995). The flow in and out of fractures is associated with a lower characteristic frequency or larger time-scale constant $\tau_f$, which depends on the size of the fractures. With increasing fracture radius, the ratio of surface area to volume decreases. Therefore, more volume of fluid has to move through an element of surface area to equalize the pressure, which requires more time. The two time-scale parameters are related to each other by the expression,

$$\tau_f = \frac{a_f}{\varsigma}\tau_m, \quad (4)$$

where $a_f$ is the fracture radius and $\varsigma$ is the grain size. $\tau_m$ is given by

$$\tau_m = \frac{c_v \eta\,(1 + K_c)}{\sigma_c k \varsigma c_1}, \quad (5)$$

where $c_v$ is the volume of an individual crack and $c_1$ is the number of connections to other elements of pore space. $\sigma_c = \pi\mu r/[2(1-\nu)]$ is the critical stress or, equivalently, the inverse of the crack space compressibility, and $K_c = \sigma_c/k_f$, where $r$ is the aspect ratio of the cracks, $\nu$ is Poisson's ratio and $k_f$ is the fluid bulk modulus.

The theory models velocity dispersion and velocity anisotropy. Thus, the anisotropy is frequency dependent. The effect is also sensitive to the fracture size. In Fig. 2, we see the change in shear-wave anisotropy with frequency as a function of fracture radius. For any given fracture size the anisotropy decreases as frequency increases. This behaviour is consistent with observations from earthquake data (Marson-Pidgeon and Savage 1997; Liu *et al*. 2001). The larger the size of the fractures, the lower the frequency range where velocity dispersion and frequency dependence of anisotropy occurs. The effect has also been observed in VSP data (Chesnokov *et al*. 2001; Liu *et al*. 2003) and will be used to invert for fracture size. Furthermore, the model can explain a large change in anisotropy due to fluid substitution for frequencies other than the static limit (Chapman *et al*. 2003). Such an effect has been found by van der Kolk *et al*. (2001) in shear-wave data from a fractured carbonate reservoir.

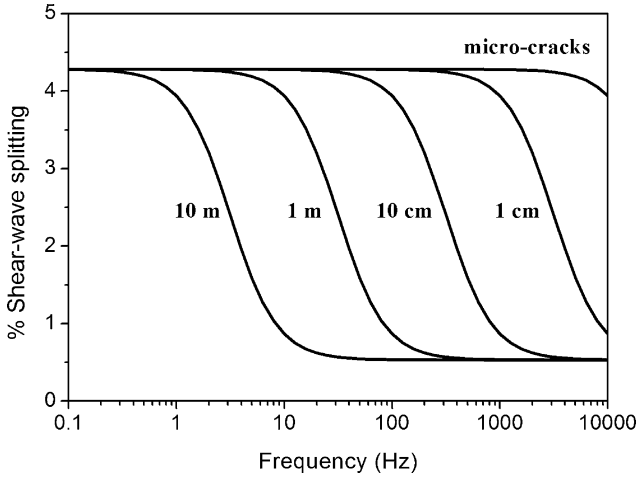


**Figure 2** Percentage of shear-wave anisotropy as a function of frequency for different fracture sizes. The waves are propagating at an angle of 60° measured from the fracture normal. For a given fracture size there is a characteristic frequency range, where anisotropy decreases with increasing frequency. For smaller fractures the change in anisotropy occurs at higher frequencies.

## CALIBRATION OF THE MODEL

Effective-medium theories for materials containing cracks or fractures can only be tested and validated by comparison with laboratory measurements. Rathore *et al.* (1995) performed measurements on synthetic sandstone samples that contained cracks of known geometry and orientation. The samples were manufactured by embedding thin metal discs into a sand-epoxy matrix, which were chemically leached out later on. P- and S-wave velocities were measured as a function of angle from the crack normal at a frequency of 100 kHz.

The data were used to test the model of Thomsen (1995) and the models of Hudson (1981) and Hudson *et al.* (1996) and to discuss their differences (Rathore *et al.* 1995; Thomsen 1995; Hudson, Pointer and Liu 2001). Rathore *et al.* (1995) and Thomsen (1995) found that for fluid-saturated samples the data are better matched by the Thomsen equant porosity model, where pressure is always equalized between cracks and equant pores, and anisotropy is therefore increased. While the Hudson (1981) model for isolated cracks gives a poor fit, the data were satisfactorily matched with the Hudson *et al.* (1996) equant porosity model, if the matrix wave speeds were also taken as fitting parameters (Hudson *et al.* 2001).

We now test the Chapman model against the data. All relevant parameters are given in Table 1. The only free variable in the modelling is the relaxation time $\tau_m$. We seek the value of $\tau_m$ that minimizes the misfit between data and model.

**Table 1** Rock and fluid parameters used in the experiment of Rathore *et al.* (1995)

| | |
|---|---|
| $V_p$ | 2678 m/s |
| $V_s$ | 1384 m/s |
| $\rho$ | 1712 kg/m$^3$ |
| $\Phi_p$ | 34.6% |
| $k_f$ | 2.16 GPa |
| $f_0$ | 100 kHz |
| Fracture density | 0.1 |
| Fracture radius | 2.75 mm |
| Aspect ratio | 0.0036 |

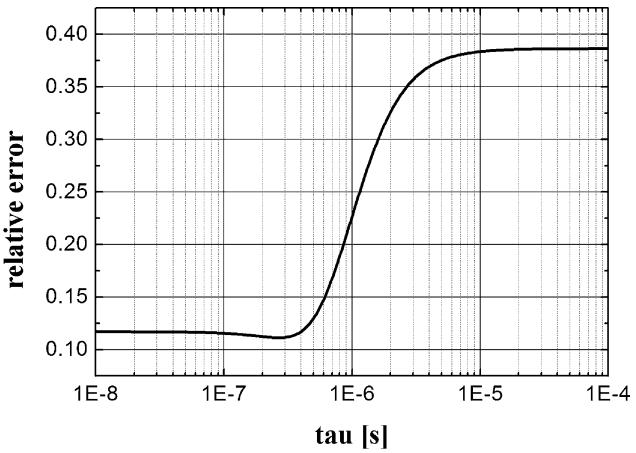


**Figure 3** Relative error between measured and modelled velocities as a function of $\tau_m$. There is a minimum at $\tau_m = 0.27$ $\mu$s. The curve also shows that the data are much better matched by a low-frequency model than a high-frequency model.

Figure 3 shows the error curve as a function of $\tau_m$. There is a minimum at $\tau_m = 0.27$ $\mu$s. This value is used to compute P- and S-wave velocities as a function of angle, and these are displayed together with the data points from Rathore *et al.* (1995) in Fig. 4. There is a good match between data and model. Figure 3 demonstrates that a low-frequency model (left side of the plot), which assumes equalized pressure throughout the pore space, fits the data much better than a high-frequency model (right side of the plot), where the cracks are effectively isolated.

The misfit for the optimal $\tau_m$ value of 0.27 $\mu$s is not significantly smaller than for the low-frequency limit. Therefore, we also attempt to model the attenuation data, which was reported by Thomsen (1995). Figures 5 and 6 show the corresponding error curve and the best-fitting model values compared with the data points. In this case the error function has a distinct minimum, which is near the optimum value obtained for the velocity modelling. Thus, we have constrained

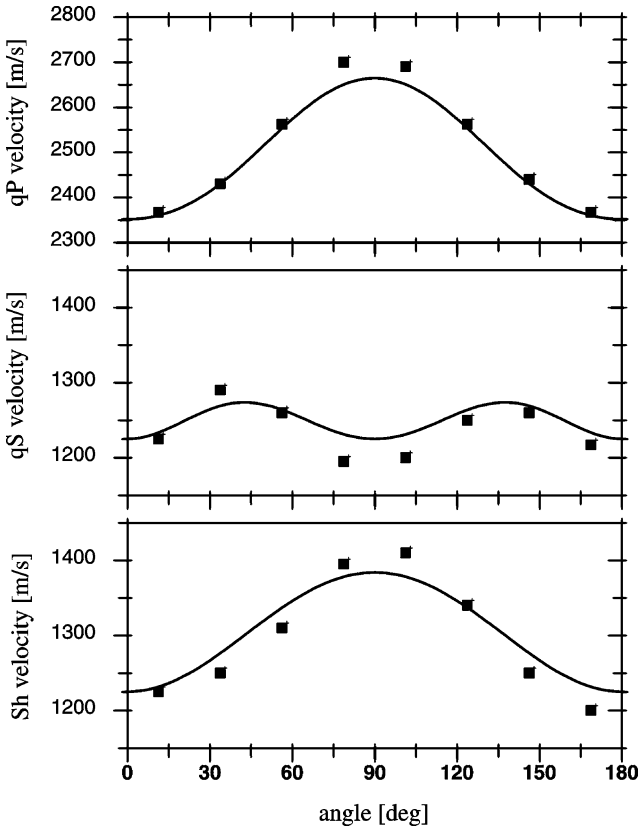


**Figure 4** Comparison of the Rathore *et al.* (1995) data (squares) for saturated synthetic sandstone with the best-fitting model. Measured and modelled velocities agree very well.

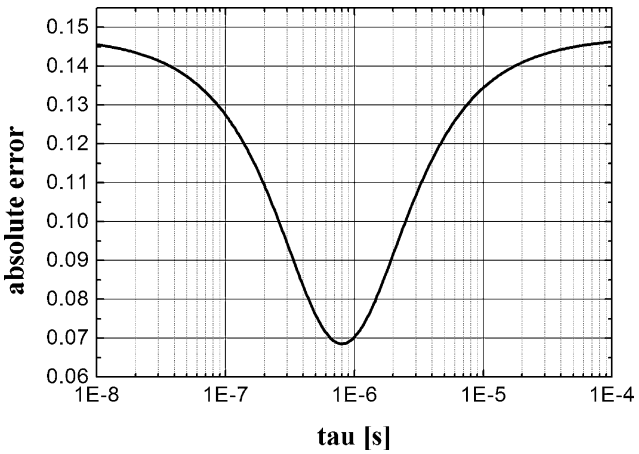


**Figure 5** Misfit between measured and modelled qP-wave attenuation as a function of $\tau_m$. There is a distinct minimum in a position similar to that in Fig. 3. This result constrains $\tau_m$ against lower values.

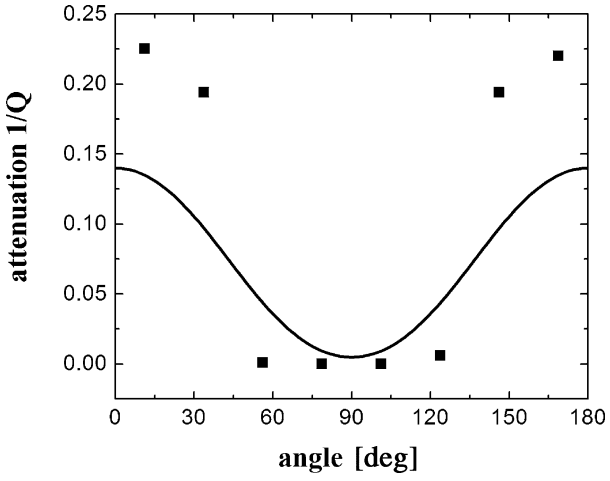


**Figure 6** Attenuation data with the best-fitting model.

$\tau_m$ against the lower-frequency limit as well. We cannot expect a perfect numerical match with the attenuation data, since scattering effects are also expected to contribute to the measured values (Hudson *et al.* 2001). The model is now tested and calibrated, and we can proceed to apply it to field data.

## APPLICATION TO FIELD DATA

We model frequency-dependent anisotropy in nine-component VSP data from the Bluebell-Altamont Field in the Uinta Basin, Utah. The aim is to estimate fracture density and fracture size from the data. The field contains a fractured gas reservoir, the Green River Formation. It is a sandstone with generally low porosity and permeability. Production from the reservoir is believed to be primarily controlled by size, orientation and concentration of natural fractures (Lynn *et al.* 1999). Therefore, estimates of these parameters from seismic data are vital information for reservoir engineers.

Fracture orientations measured from seismic data, boreholes, outcrops and cores show a fracture strike between N30°W and N45°W. Observed fractures are vertical to subvertical. The VSP is a near-offset VSP with the source located 550 ft west of the well. Three-component receivers were placed at depths from 2800 ft to 8650 ft with a 50 ft spacing. The reservoir (Green River Formation) is located at depths of 6687 ft to 8591 ft. A P-wave and two orthogonal S-wave sources were used, yielding a nine-component data set.

Shear-wave splitting has been observed in the VSP data and analysed from direct arrivals. The polarization angles of the fast shear waves are found to be consistent at N43°W throughout all receiver depths. This direction is identified with the fracture strike. The time delay between the fast and the slow shear waves shows a sharp increase with depth at the reservoir level, indicating the presence of fractures.

We now analyse the data from the Green River Formation for frequency-dependent shear-wave splitting as described by Chesnokov *et al*. (2001) and Liu *et al*. (2003). Following Liu *et al*. (2003), the data are first filtered into several frequency bands. Then we perform an Alford rotation to determine the polarization angles of the fast shear-wave component. The time delays are obtained by cross-correlating the rotated traces. The processing technique has been tested on synthetic data for both frequency-dependent and frequency-independent anisotropic materials to ensure that the effects described below are not related to processing issues (Liu *et al*. 2003).

Figures 7 and 8 show the results. The polarization angles are consistent at around 43° for all frequency bands. The time delays, in contrast, show a systematic variation with frequency: as frequency increases, the change in time delay with depth decreases, i.e. the magnitude of anisotropy decreases. This behaviour will be used to invert for fracture density and fracture radius.

Before we can proceed to the inversion, we have to correct the $\tau_m$ value obtained from the calibration to laboratory measurements in order to match the rock and fluid properties of the Green River Formation. The latter are given in Table 2. The Rathore *et al*. (1995) experiment was performed on water-saturated high-porosity sandstone, while the Green River Formation is a gas-saturated sandstone of low porosity. From (5) we can see that $\tau_m$ is proportional to the fluid viscosity $\eta$, multiplied by the term $(1/\sigma_c + 1/k_f)$. There is a large change in viscosity and fluid bulk modulus going from water to natural gas. Since all relevant parameters are known, we can calculate the corresponding change in $\tau_m$.

Also, $\tau_m$ is inversely proportional to the permeability. Since we do not know the permeability values for either case, we suggest inferring the change in permeability from the change in porosity. For that purpose we use an extended form of the Kozeny–Carman relationship given by Mavko and Nur (1997), which considers the existence of a percolation threshold. As a result we obtain a decrease in permeability and therefore an increase in $\tau_m$ of a factor of 123. Combining all corrections yields a $\tau_m$ value of 6 $\mu$s, which can now be used for modelling the elastic response of the Green River sandstone.

From the polarization angles obtained from the field data we infer an average fracture strike of N43°W, which is input

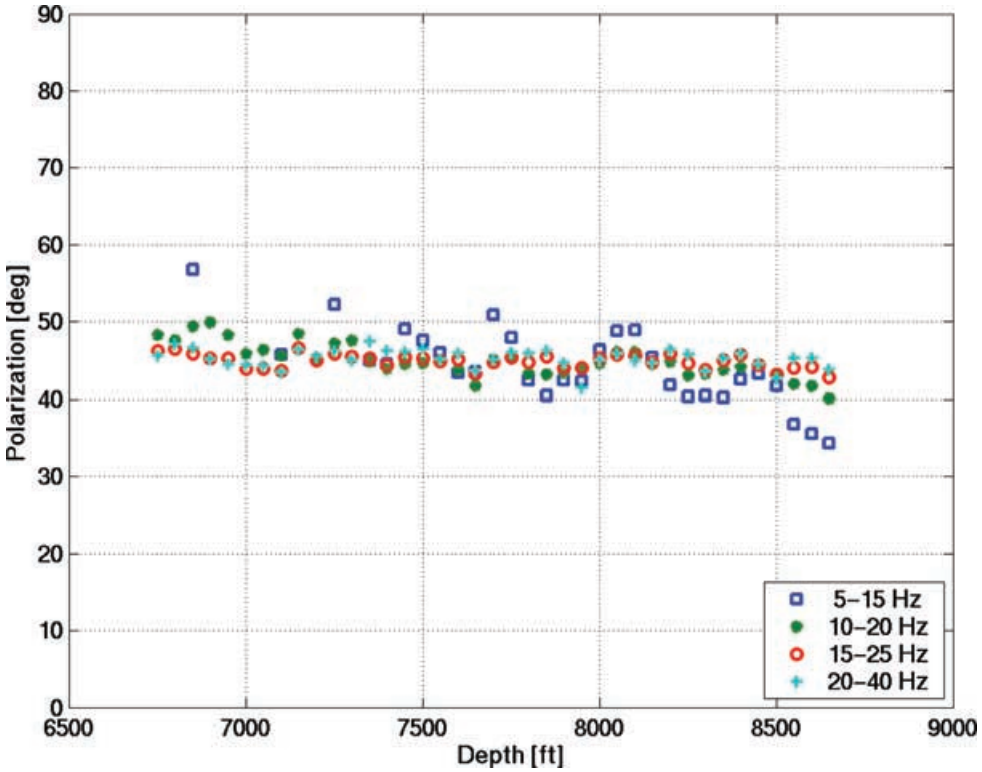


**Figure 7** Polarization angles of the fast shear wave for different frequency bands. The values are consistent around 43°, which agrees with the fracture strike in the reservoir.

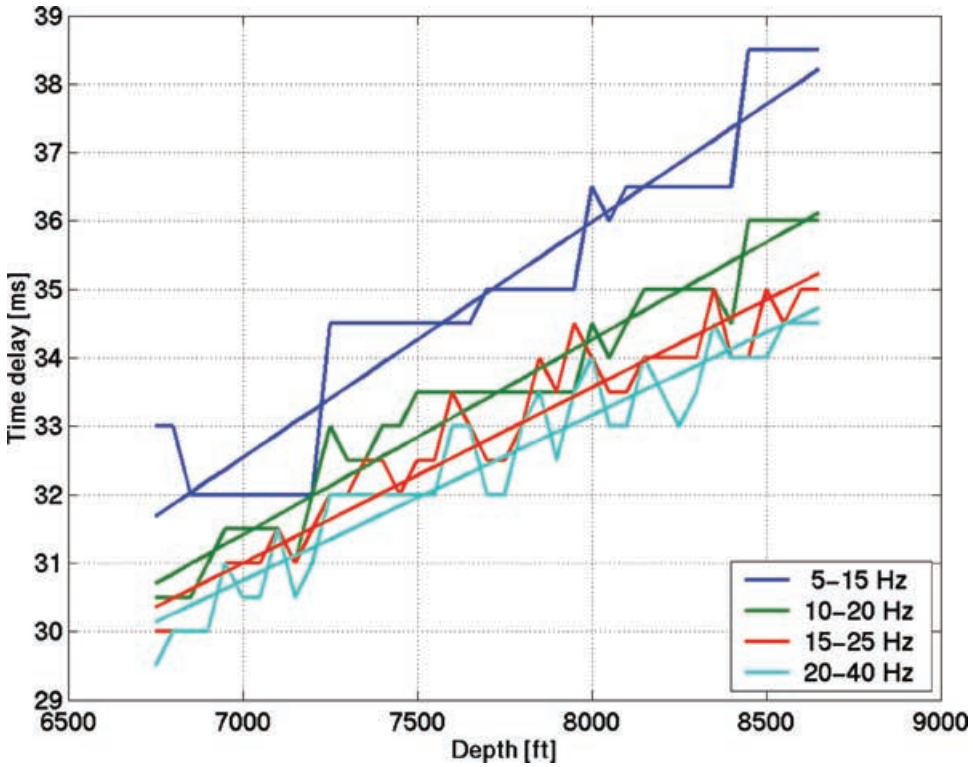


**Figure 8** The time delays over the reservoir depth interval show a systematic decrease with increasing frequency.

**Table 2** Rock properties of the Green River Formation in the Bluebell-Altamont Field

| | |
|---|---|
| $V_p$ | 4877 m/s |
| $V_s$ | 2575 m/s |
| $\rho$ | 2600 kg/m$^3$ |
| $\Phi_p$ | 9.4% |
| $k_f$ | 25 MPa |

into the model. The aspect ratio is chosen to be very small with a value of 0.0001, so that its exact value has no influence on the resulting elastic constants. The value is supported by observations from borehole images and cores (Lynn *et al.* 1995). We tilt the fractures by 20° from the vertical in order to model propagation directions of the waves, where frequency-dependent effects would occur. In reality there would be a distribution of orientations around a certain angle that would produce the effect. Slightly tilted fractures have also been observed in the field (Lynn *et al.* 1995).

Now the only unknowns in the model are fracture density and fracture radius. We estimate these parameters by matching the change in time delay with frequency, which was observed in the data. For each pair of fracture density and fracture radius we compute the RMS error between the measured and the predicted increases in time delay with depth as a function of frequency.

Figure 9 displays the error function. There is a well-defined minimum at a fracture radius of about 3 m and a fracture density of approximately 3.5%. It is interesting to observe the bottom and top sections of the diagram. They represent what would be obtained using the Thomsen (1995) and Hudson (1981) models, respectively. As stated earlier, neither of the models is sensitive to the fracture size, which can be clearly seen in Fig. 9. Furthermore, we would infer a fracture density of 5% from the data by using Hudson's model, while the model of Thomsen yields a value of about 2.5%. However, by incorporating the frequency-dependent effects and modelling the data with Chapman's (2003) model, we obtain a more tightly constrained estimate of the fracture density, and we can also deduce a fracture size from the data.

The two fracture parameters (i.e. fracture radius and fracture density) are used to carry out forward modelling. We create a simple four-layer model that matches the main formations in the field. The model parameters are given in Table 3. Synthetic seismograms are computed using the reflectivity method, which has been modified to handle

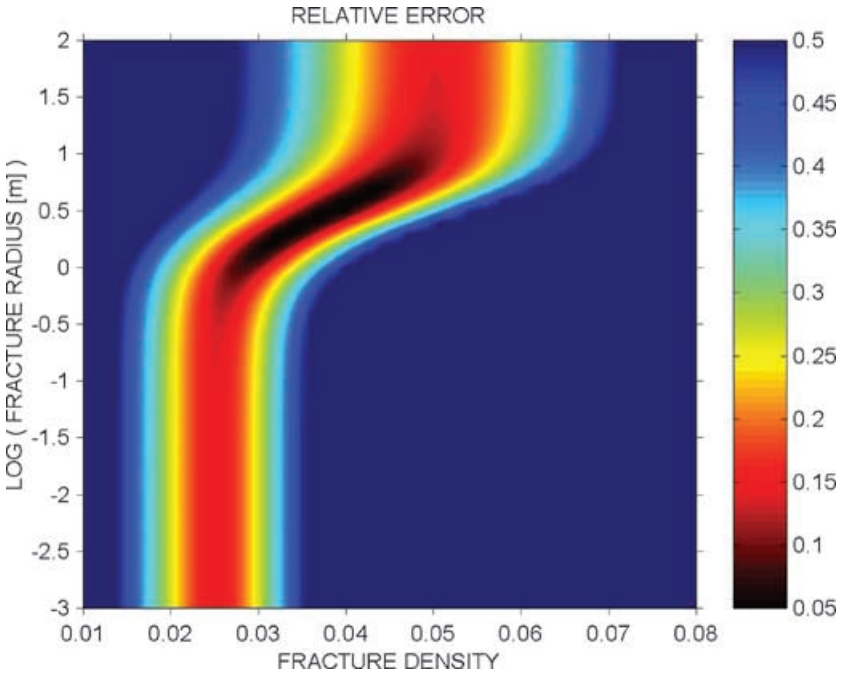


**Figure 9** Relative error between measured and computed time delays as a function of frequency for a wide range of fracture densities and fracture sizes. There is a clear minimum at a fracture density of 0.035 and a fracture radius of about 3 m.

**Table 3** Parameters of the model that are used to generate synthetic seismograms

| Depth (ft) | $\rho$ (kg/m$^3$) | $V_p$ (m/s) | $V_s$ (m/s) | |
|---|---|---|---|---|
| 2800 | 2200 | 2963 | 1363 | Anisotropic |
| 6687 | 2450 | 4000 | 2128 | Isotropic |
| 8591 | 2600 | 4877 | 2575 | Anisotropic, frequency-dependent |
| Half-space | 2500 | 4382 | 2583 | Isotropic |

frequency-dependent anisotropic elastic constants. The four-component shear-wave data are shown in Fig. 10 before and after an Alford rotation and can be compared with the synthetics in Fig. 11. We process the synthetic data in the same way as the real data. The polarization angles of the fast shear wave are plotted in Fig. 12 for different frequency bands. They are invariant to frequency and plotted at a constant value of 43°, which is the fracture strike that was input into the model. From the measured time delays we can compute the percentage of anisotropy. Figure 13 shows the modelled percentage of anisotropy as a function of frequency compared with the real data results. There is good agreement between the two curves. The error bars represent the error between measured time delays as a function of depth and the best-fitting straight line.

Finally, we compare our deduced fracture radius of about 3 m (or fracture length of 6 m) with independent borehole data. There is evidence from borehole images and cores that lengths of fractures in the reservoir lie in the range of 2–3 m (Lynn *et al*. 1995). Our inferred average length matches these independent observations quite closely.

## DISCUSSION

Conventional static equivalent-medium theories can be used to infer an average fracture density and orientation from measurements of seismic anisotropy. However, the models fail to provide any information on the fracture size. Moreover, there is evidence of frequency-dependent anisotropy from field data that cannot be satisfactorily explained by static equivalent-medium theories.

Heterogeneous and fractured porous rock may be characterized by observations in different critical wavelength ranges, each reflecting different physical mechanisms. The scale length associated with the heterogeneities or the fracturing has to be much smaller than the seismic wavelength to cause effective anisotropy instead of scattering.

Scattering of seismic waves due to aligned heterogeneities has long been recognized to be frequency dependent (e.g. Shapiro and Hubral 1995; Werner and Shapiro 1999). Shapiro and Hubral (1995) have shown that in finely layered media velocity dispersion and frequency-dependent anisotropy in the seismic frequency band can be produced by scattering, if there is a specific ratio between wavelength and

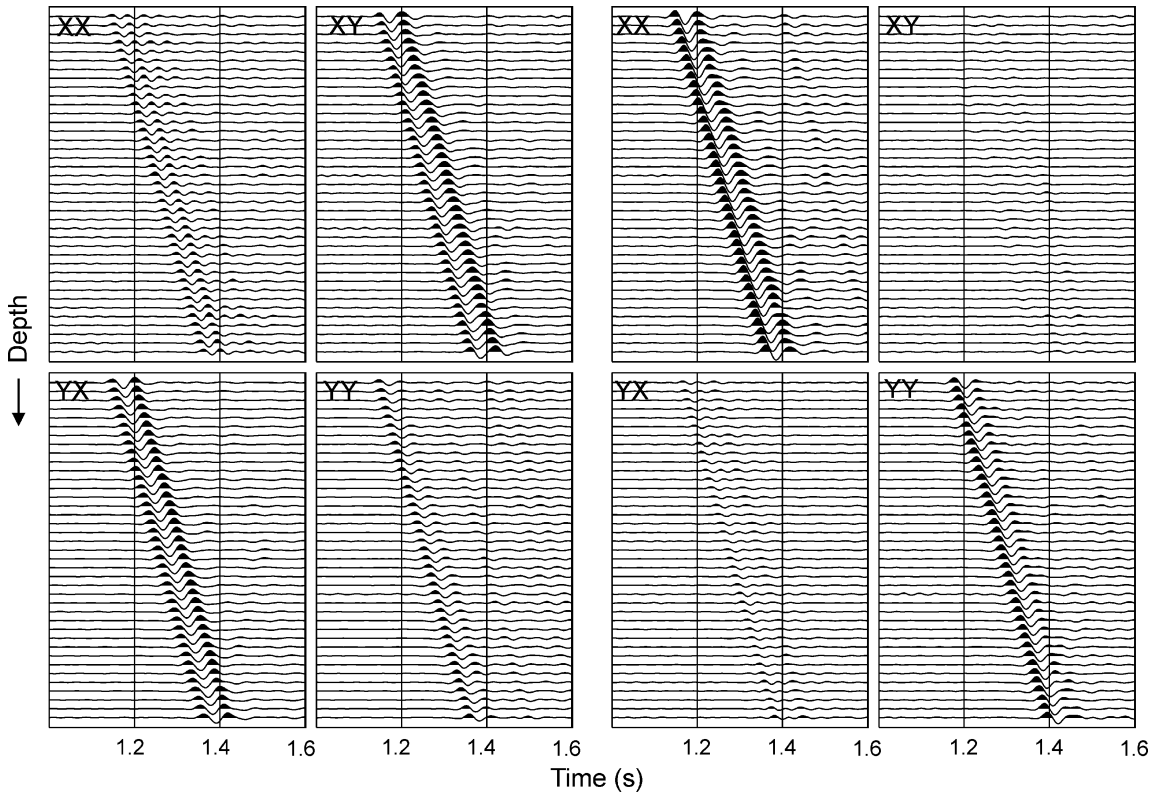


**Figure 10** Four-component shear-wave data before (left) and after (right) Alford rotation. The strong energy in the cross-diagonal components before rotation indicates shear-wave splitting.

correlation length. They predict significant frequency-dependent shear-wave splitting at far offsets. The data set investigated in this study, however, is a near-offset VSP with nearly vertical incidence. The effect of layering does not cause shear-wave splitting at normal incidence and therefore cannot explain the observed shear-wave behaviour.

The model of Chapman (2003) as used here predicts frequency-dependent anisotropy due to squirt flow in fractured porous rock. The fractures can be much larger than the cracks and pores, but are much smaller than the wavelength. The explicit dependence on fracture size is in contrast to the earlier models of Hudson *et al*. (1996) and Thomsen (1995). Tod and Liu (2002) modelled frequency-dependent anisotropy in earthquake and VSP data using a layer-bounded fracture model based on Hudson *et al*. (1996). Nevertheless, it appears that in this study rather high values of the permeability had to be assumed, and it remains an open question as to whether these values are reasonable.

In the model of Chapman (2003), coupled fluid-flow motion occurs on two scales: the grain scale and the scale of the fractures. As a consequence the form of the predicted frequency dependence of anisotropy is directly related to the fracture size. Previous estimates of the squirt-flow frequency have given high values, typically between the sonic and ultrasonic bands, which leads to the suggestion that at seismic frequencies there should be little dispersion (Thomsen 1995). In the presence of larger-scale fractures, however, substantial frequency dependence can be expected in the seismic frequency ranges, and therefore it is not safe to treat seismic frequency as a low-frequency limit.

Our study has an important implication for the characterization of natural fractures in that fracture sizes, which control the fluid flow, may potentially be predicted from seismic anisotropic measurement. This goes beyond applications of static equivalent-medium theories that are limited to extracting information about fracture orientation and fracture density.

## CONCLUSIONS

We have presented results demonstrating the dependence of seismic anisotropic parameters on frequency using a recently

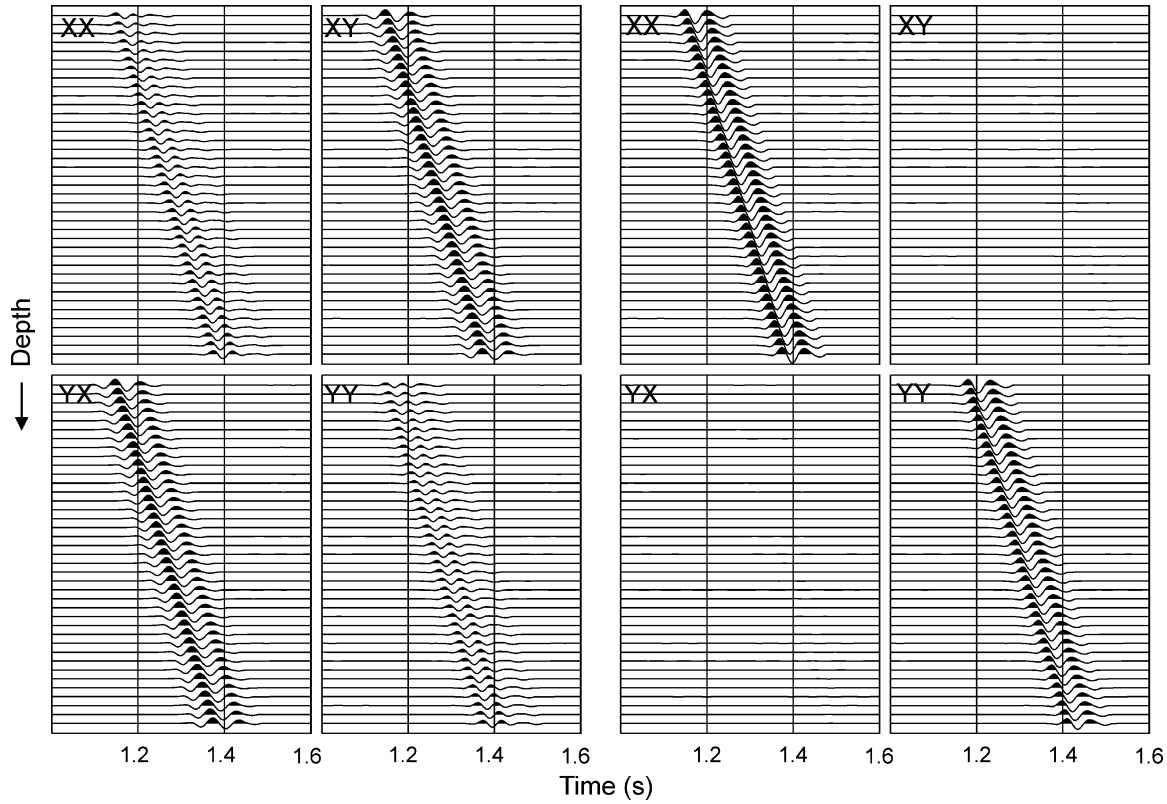


**Figure 11** Four-component synthetics before and after Alford rotation. They agree well with the real data.

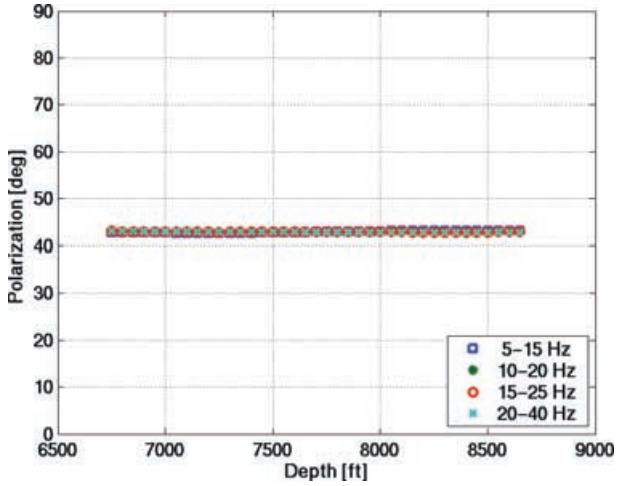


**Figure 12** Polarization angles measured from the synthetic data for different frequency bands. The values are constant at 43° for all frequencies, which corresponds to the fracture strike in the reservoir layer.

developed dynamic equivalent-medium theory by Chapman (2003) and Chapman *et al*. (2003). This model is based on a squirt-flow mechanism and suggests that frequency dependence of anisotropy is sensitive to the length scale of fractures. We have tested and calibrated the model against published laboratory data. This provides the basis for application to field data. We developed a methodology for using the model to invert for fracture density and fracture size from frequency-dependent shear-wave splitting in a near-offset VSP. The derived average fracture length matches geological evidence very well.

Since the analysed data set is a near-offset VSP with nearly vertical incidence, scattering due to thin layers can be excluded as a cause of the observed shear-wave behaviour. If the measured frequency-dependent anisotropy was caused by scattering at fractures, then the dominant length scales associated with the fracturing would have to be of the order of seismic wavelengths, i.e. several tens to hundreds of metres. We believe that the squirt-flow mechanism is more likely to be the dominant cause, which is supported by the good match between inferred fracture length and independent geological data. Moreover, there is evidence from field and laboratory data that fluid plays a significant role with regard to velocity dispersion and attenuation (Spencer 1981; van der Kolk *et al*. 2001; Parra, Hackert and Xu 2002).

The study demonstrates that the frequency dependence of shear-wave splitting can be extracted from seismic data and

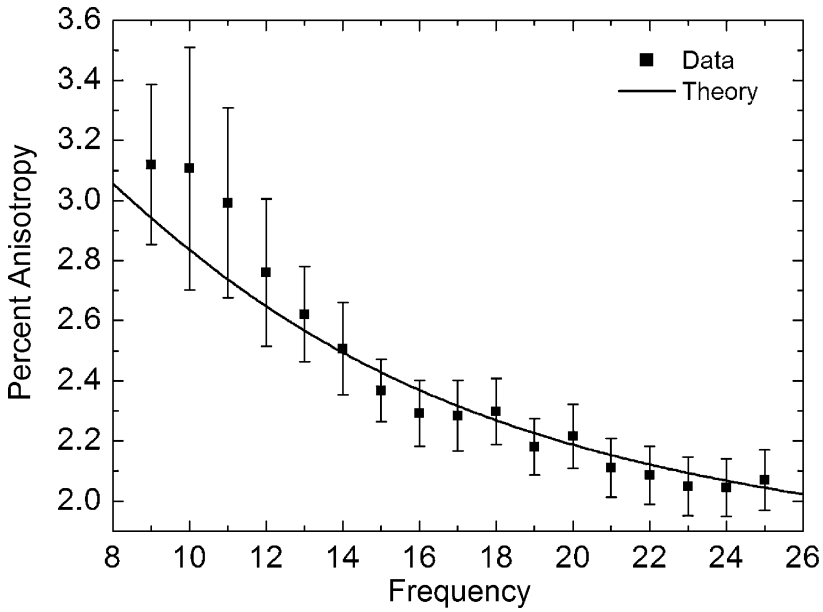


**Figure 13** Percentage anisotropy as a function of frequency measured from the VSP data, compared with the modelled results.

interpreted in terms of an average length scale of fractures. The most important result is the successful discrimination between the effect of microcracks at the grain or millimetre scale and the effect of formation-scale fractures. Fluid flow and permeability in a reservoir are believed to be much more strongly controlled by formation-scale fractures than by microcracks.

Our study indicates that there is great potential in using frequency-dependent seismic anisotropy to estimate average fracture sizes, which are ultimately needed in reservoir simulation. It is the aim of future work to extend our approach to the use of other attributes, such as amplitudes and attenuation, and to understand better the effects of multiscale fractures on amplitudes versus offsets and frequency variation with offset as used by Lynn *et al*. (1999). With further validation of the model there is potential for an improved and more quantitative fracture characterization from seismic data compared with previous approaches using static theory.

## ACKNOWLEDGEMENTS

We thank John Queen (ConocoPhillips) and Heloise Lynn (Lynn Inc.) for useful discussions and for providing the field VSP data (by H.L.). We also thank Simon Tod (formerly at BGS, now at BP) and John Hudson (Cambridge University) for many discussions about the fracture modelling and for comments on this work. We are very grateful to David Taylor (Edinburgh University) for his help with the computation of synthetic seismograms (using a modified ANISEIS package). This work is supported by the Natural Environment Research Council (UK) as part of the 'Thematic micro-to-Macro Programme' (Project No. GST22305), and by the sponsors of the Edinburgh Anisotropy Project (EAP). This paper is published with the approval of the Executive Director of the British Geological Survey (NERC) and the EAP sponsors: ENI-Agip, BP, BG Group, ChevronTexaco, CNPC, ConocoPhillips, ExxonMobil, Norsk Hydro, KerrMcGee, Marathon, PetroChina, PGS, Schlumberger, Total, Trade Partners UK and Veritas DGC.

## REFERENCES

Brown R. and Korringa J. 1975. On the dependence of the elastic properties of a porous rock on the compressibility of the pore fluid. *Geophysics* **40**, 608–616.

Chapman M. 2000. *Modelling the wide-band laboratory response of rock samples to fluid and pressure changes*. PhD thesis, University of Edinburgh.

Chapman M. 2003. Frequency-dependent anisotropy due to mesoscale fractures in the presence of equant porosity. *Geophysical Prospecting* **51**, 369–379.

Chapman M., Maultzsch S., Liu E. and Li X.Y. 2003. The effect of fluid saturation in an anisotropic, multi-scale equant porosity model. *Journal of Applied Geophysics*, in press (10IWSA Proceedings).

Chapman M., Zatsepin S.V. and Crampin S. 2002. Derivation of a microstructural poroelastic model. *Geophysical Journal International* **151**, 427–451.

Chesnokov E.M., Queen J.H., Vichorev A., Lynn H.B., Hooper J., Bayuk I., Castagna J. and Roy B. 2001. Frequency dependent anisotropy. 71st SEG Meeting, San Antonio, Texas, USA, Expanded Abstracts, 2120–2123.

Crampin S. 1985. Evaluation of anisotropy by shear-wave splitting. *Geophysics* **50**, 142–152.

Eshelby J.D. 1957. The determination of the elastic field of an ellipsoidal inclusion and related problems. *Proceedings of the Royal Society of London* **A241**, 376–396.

Hudson J.A. 1981. Wave speeds and attenuation of elastic waves in material containing cracks. *Geophysical Journal of the Royal Astronomical Society* **64**, 133–150.

Hudson J.A., Liu E. and Crampin S. 1996. The mechanical properties of materials with interconnected cracks and pores. *Geophysical Journal International* **124**, 105–112.

Hudson J.A., Pointer T. and Liu E. 2001. Effective-medium theories for fluid-saturated materials with aligned cracks. *Geophysical Prospecting* **49**, 509–522.

van der Kolk C.M., Guest W.S. and Potters J.H.H.M. 2001. The 3D shear experiment over the Natih field in Oman: the effect of fracture-filling fluids on shear propagation. *Geophysical Prospecting* **49**, 179–197.

Li X.Y. 1997. Fractured reservoir delineation using multicomponent seismic data. *Geophysical Prospecting* **45**, 39–64.

Liu E., Crampin S., Queen J.H. and Rizer W.D. 1993. Velocity and attenuation anisotropy caused by microcracks and macrofractures in a multiazimuthal reverse VSP. *Canadian Journal of Exploration Geophysics* **29**, 177–188.

Liu E., Hudson J.A. and Pointer T. 2000. Equivalent medium representation of fractured rock. *Journal of Geophysical Research* **105**(B2), 2981–3000.

Liu E., Queen J.H., Li X.Y., Chapman M., Maultzsch S., Lynn H.B. and Chesnokov E.M. 2003. Observation and analysis of frequency-dependent anisotropy from a multicomponent VSP at Bluebell-Altamont Field, Utah. *Journal of Applied Geophysics*, in press (10IWSA Proceedings).

Liu K., Zhang Z., Hu J. and Teng J. 2001. Frequency band-dependence of S-wave splitting in China mainland and its implications. *Science in China (Series D)* **44**(7), 659–665.

Lucet N. and Zinszner B. 1992. Effects of heterogeneities and anisotropy on sonic and ultrasonic attenuation in rocks. *Geophysics* **57**, 1018–1026.

Lynn H.B., Bates C.R., Hoekstra P., Simone M.K. and Phillips D.R. 1995. *Fracture Detection, Mapping, and Analysis of Naturally Fractured Gas Reservoirs using Seismic Technology*. Report to the US Department of Energy.

Lynn H.B., Beckham W.E., Simon K.M., Bates C.R., Layman M. and Jones M. 1999. P-wave and S-wave azimuthal anisotropy at a naturally fractured gas reservoir, Bluebell-Altamont field, Utah. *Geophysics* **64**, 1312–1328.

Marson-Pidgeon K. and Savage M.K. 1997. Frequency-dependent anisotropy in Wellington, New Zealand. *Geophysical Research Letters* **24**, 3297–3300.

Mavko G. and Nur A. 1997. The effect of a percolation threshold in the Kozeny–Carman relation. *Geophysics* **62**, 1480–1482.

Mueller M.C. 1992. Using shear waves to predict lateral variability in vertical fracture intensity. *The Leading Edge* **11**(2), 29–35.

Murphy W.F. 1985. Sonic and ultrasonic velocities: Theory versus experiment. *Geophysical Research Letters* **12**, 85–88.

Nishizawa O. 1982. Seismic velocity anisotropy in a medium containing oriented cracks – transversely isotropic case. *Journal of Physics of the Earth* **30**, 331–347.

Parra J.O., Hackert C.L. and Xu P.C. 2002. Characterization of fractured low Q zones at the Buena Vista Hills reservoir, California. *Geophysics* **67**, 1061–1070.

Potters J.H.H.M., Groenendaal H.J.J., Oates S.J., Hake J.H. and Kalden A.B. 1999. The 3D shear experiment over the Natih field in Oman: Reservoir geology, data acquisition and anisotropy analysis. *Geophysical Prospecting* **47**, 637–662.

Queen J.H. and Rizer W.D. 1990. An integrated study of seismic anisotropy and the natural fracture systems at the Conoco Borehole Test Facility, Kay County, Oklahoma. *Journal of Geophysical Research* **95**, 11255–11273.

Queen J.H., Rizer W.D. and DeMartini D. 1992. Geophysical methods of fracture detection and estimation. *The Leading Edge* **11**, 19–21.

Rathore J.S., Fjaer E., Holt R.M. and Renlie L. 1995. P- and S- wave anisotropy of a synthetic sandstone with controlled crack geometry. *Geophysical Prospecting* **43**, 711–728.

Schoenberg M. 1980. Elastic wave behaviour across linear slip interfaces. *Journal of the Acoustical Society of America* **68**, 1516–1521.

Shapiro S.A. and Hubral P. 1995. Frequency-dependent shear-wave splitting and velocity anisotropy due to elastic multilayering. *Journal of Seismic Exploration* **4**, 151–168.

Spencer J.W. 1981. Stress relaxation at low frequencies in fluid-saturated rocks: Attenuation and modulus dispersion. *Journal of Geophysical Research* **86**, 1803–1812.

Thomsen L. 1995. Elastic anisotropy due to aligned cracks in porous rock. *Geophysical Prospecting* **43**, 805–829.

Tod S.R. 2001. The effects on seismic waves of interconnected nearly aligned cracks. *Geophysical Journal International* **146**, 249–263.

Tod S.R. and Liu E. 2002. Frequency-dependent anisotropy due to fluid flow in bed limited cracks. *Geophysical Research Letters* **29**(15), 39-1–39-4. Paper no. 10.1029/2002GL015369.

Werner U. and Shapiro S.A. 1999. Frequency-dependent shear-wave splitting in thinly layered media with intrinsic anisotropy. *Geophysics* **64**, 604–608.

Winkler K.W. 1986. Estimates of velocity dispersion between seismic and ultrasonic frequencies. *Geophysics* **51**, 183–189.